Miner Deposita
DOI 10.1007/s00126-015-0602-3

ARTICLE

Variation of molybdenum isotopes in molybdenite from porphyry and vein Mo deposits in the Gangdese metallogenic belt, Tibetan plateau and its implications

Yong Wang[1] · Lian Zhou[1] · Shan Gao[1] · Jian-Wei Li[1] · Zhi-Fang Hu[1] · Lu Yang[2] · Zhao-Chu Hu[1]

Received: 26 October 2014 / Accepted: 1 July 2015

Abstract We present Mo isotopic ratios of molybdenite from five porphyry molybdenum deposits (Chagele, Sharang, Jiru, Qulong, and Zhuonuo) and one quartz-molybdenite vein-type deposit (Jigongcun) along the Gangdese metallogenic belt in the Tibetan Plateau. These deposits represent a sequence of consecutive events of the India-Asia collision at different periods. Additional molybdenite samples from the Henderson Mo deposit (USA), the oceanic subduction-related El Teniente (Chile), and Bingham (USA) porphyry Cu-(Mo) deposits were analyzed for better understanding the controls on the Mo isotope systematics of molybdenite. The results show that molybdenite from Sharang, Jiru, Qulong, and Zhuonuo deposits have similar δ^{97}Mo (~0‰), in agreement with the values of the Henderson Mo deposit (−0.10‰). In contrast, samples from the Changle and Jigongcun deposit have δ^{97}Mo of 0.85‰ to 0.88‰ and −0.48 ‰, respectively. Molybdenite from the El Teniente and Bingham deposits yields intermediate δ^{97}Mo of 0.27 and 0.46‰, respectively. The Mo isotopes, combined with Nd isotope data of the ore-bearing porphyries, indicate that source of the ore-related magmas has fundamental effects on the Mo isotopic compositions of molybdenite. Our study indicates that molybdenite related to crustal-, and mantle-derived magmas has positive or negative δ^{97}Mo values, respectively, whereas molybdenite from porphyries formed by crust-mantle mixing has δ^{97}Mo close to 0‰. It is concluded that the Mo isotope composition in the porphyry system is a huge source signature, without relation to the tectonic setting under which the porphyry deposits formed.

Keywords Molybdenite · Molybdenum isotope · Gangdese · Tibetan Plateau

Editorial handling: R.L. Romer

✉ Lian Zhou
zhcug@163.com

[1] State Key Laboratory of Geological Processes and Mineral Resources, China University of Geosciences, Wuhan 430074, China

[2] Chemical Metrology, Institute for National Measurement Standards, National Research Council Canada, Ottawa, Ontario K1A 0R6, Canada

Introduction

Mo isotopes have been increasingly used as an indicator for paleoclimate on the Earth (Siebert et al. 2003; Arnold et al. 2004; Lehmann et al. 2007; Pearce et al. 2008; Zhou et al. 2012; Xu et al. 2012, 2013). For example, it has a great potential in recording the redox condition of the ocean through time (Arnold et al. 2004; Wille et al. 2007), which is essential for better understanding marine carbonate equilibria and pH of paleo-ocean. Molybdenite is an important ore mineral in many porphyry Cu-Mo systems (e.g., Cooke et al. 2005; Hou et al. 2009), as well as one of the most significant reservoirs for molybdenum in continental crust. However, Mo isotopes in molybdenite have been rarely studied, and the previous limited studies aimed to determine the isotopic compositions of molybdenite formed under different conditions, including porphyry, skarn, metamorphism, Fe-oxide, and epithermal polymetallic veins deposit (Barling et al. 2001; Pietruszka et al. 2006; Malinovsky et al. 2007; Hannah et al. 2007; Mathur et al. 2010). The fractionation mechanism of Mo isotopes during mineralization remains poorly understood. Results from Malinovsky et al. (2007) indicate that Mo isotopes of molybdenite do not show any correlations with formation age or temperature in magmatic-hydrothermal systems. Hannah et al. (2007) analyzed 20 samples from different types of deposits representing different ages and ore-forming

Published online: 15 July 2015

temperatures. They found that the Mo isotopic composition was not related to the crystallization temperature, age, geographic distribution, as well as geologic conditions. Consequently, they proposed that fractionation of Mo isotope in molybdenite is largely controlled by Rayleigh distillation. Mathur et al. (2010) reported a variation of Mo isotopes in molybdenites from different types of high-temperature hydrothermal ore deposits, with δ^{97}Mo ranging from −0.53 to 0.53 ‰ in porphyry, 0.31 to 1.34‰ in iron oxide-Cu-Au, and −0.24 to 0.65‰ in skarn deposits, respectively. The observed variations likely reflect the fractionation of Mo isotopes into different mineral phases during the ore-forming processes (Mathur et al. 2010). During the formation of the ore, it has yet to be investigated whether the Mo isotopic composition of molybdenite is related to the source of ore-related magmas and the tectonic setting.

In this study, 14 molybdenite samples from 8 porphyry Cu-Mo deposits formed in distinct tectonic environment were analyzed. The aim of this study is to investigate possible correlations between Mo isotopes, source of ore magmas, and tectonic setting responsible for the magmatic-hydrothermal mineralization. In total, 11 samples were collected from 5 porphyry molybdenum deposits (Chagele, Sharang, Jiru, Qulong, and Zhuonuo) and a quartz-molybdenite vein-type deposit (Jigongcun) from the Gangdese metallogenic belt in the Tibetan Plateau. The Gangdese metallogenic belt has been interpreted as a result of the continental collision between the Indian and Asian Plates (Hou et al. 2013). The ages of these deposits range from 65 to 10 Ma, spanning the entire orogenic and post-collisional history. Three other samples were analyzed for comparison, each from the Henderson porphyry Mo deposit in the USA, and two porphyry Cu-Mo deposits in Chile (El Teniente) and the USA (Bingham). The results, combined with Nd isotope data of the ore-related intrusions, are used to investigate the potential of Mo isotopes in molybdenite as an indicator of tectonic setting of mineralization and source of ore-related magmas.

Geological setting

The Tibetan plateau is composed of four blocks or terranes: the Songpan-Ganze, Qiangtang, Lhasa terrane, and the Himalaya, from north to south (Hou et al. 2009). These blocks are bounded by the Jinsha (JS), Bangong-Nujiang (BNS), and Indo-Yarlung sutures (IYS) (Fig. 1a). The Gangdese metallogenic belt is located between the BNS and IYS (Fig. 1b). It is formed as a result of the Indian-Asian continental collision during the early Cenozoic. It is widely believed that the Lhasa terrane was a part of the Gondwana supercontinent during the Triassic to mid-late Jurassic, and then drifted northwards to collide with the Qiangtang terrane (Yin and Harrion 2000). The Lhasa terrane is composed of the mid-Proterozoic to early Cambrian basement that is unconformably overlain by the Ordovician to Triassic shallow marine clastic and carbonate rocks (Hou et al. 2009). It has undergone a complex tectonic evolution since the northward subduction of the Neo-Tethyan ocean in the Cretaceous (Chung et al. 2005) that formed the IYS and the Andes-type Gangdese arc batholiths (Chu et al. 2006; Zhu et al. 2009). The India-Asia collision at around 65 Ma (Ding et al. 2003) has led to two major episodes of magmatic activity along the Gangdese belt, forming voluminous syn-collisional (65~38 Ma) and post-collisional (26~10 Ma) granitic intrusions.

The Gangdese metallogenic belt can be subdivided into the Northern, Central, and Southern belts, separated by the Shiquan River-Nam Tso Melang Zone (SNMZ) and Luobadui-Milashan Fault (LMF) from north to south (Fig. 1; Zhu et al. 2009, 2011). Geochemical and isotopic constraints from the granitic intrusions indicate that the Northern and Southern Gangdese belts are characterized by a juvenile lower crust, whereas the Central belt is underlain by an ancient lower crust (Zhu et al. 2011). Numerous Pb-Zn-Cu-Mo-W polymetallic deposits are developed in the Gangdese metallogenic belt (Hou et al. 2009, 2013). The Jiru, Zhunuo and Qulong, and Jigongcun Mo deposits are located in the Southern Gangdese belt, whereas the Chagele and Sharang deposits are in the Central Gangdese belt (Fig. 1).

Mo deposits from Tibetan plateau

The Chagele porphyry Cu-Mo deposit is located in Ngamring County, Xigaze region, Tibet. Mineralization is hosted in a granite porphyry, which intrudes phyllite and quartz sandstone of the Middle Permian Xiala Formation at ca. 63.3±0.8 Ma (Gao et al. 2012). Molybdenite and chalcopyrite are the main ore minerals, occurring mostly in veins coexisting with variable amounts of chalcopyrite, pyrite, and quartz (Gao et al. 2012). Five molybdenite samples yielded a Re-Os isochronal age of 61.5±0.6 Ma that is consistent with the zircon U-Pb age (63.3±0.8 Ma) of the ore-hosting porphyry (Gao et al. 2012).

The Jiru porphyry Cu-Mo deposit is located in Namling County, Xigaze region, Tibet. It is hosted in a monzogranite intrusion dated at 48.6±0.8 Ma, which is intruded by a 16.0± 0.4 Ma monzogranite porphyry (Zheng et al. 2014). The ore-related alteration is dominated by an inner K-silicate zone and an outer quartz-sericite zone, both locally overprinted by propylitic alteration. Chalcopyrite and molybdenite are the predominant ore minerals, with minor amounts of pyrite, galena, and sphalerite. Five molybdenite separates gave an isochron age of 44.9±2.6 Ma (Zheng et al. 2014).

The Zhuonuo porphyry Cu-Mo deposit is located in Ngamring County, Xigaze region, Tibet. The ore-related granite is emplaced into intermediate-silicic volcanic and pyroclastic rocks of the Paleogene Linzizong Formation along NE-striking faults (Zheng et al. 2007). There are three mineralized

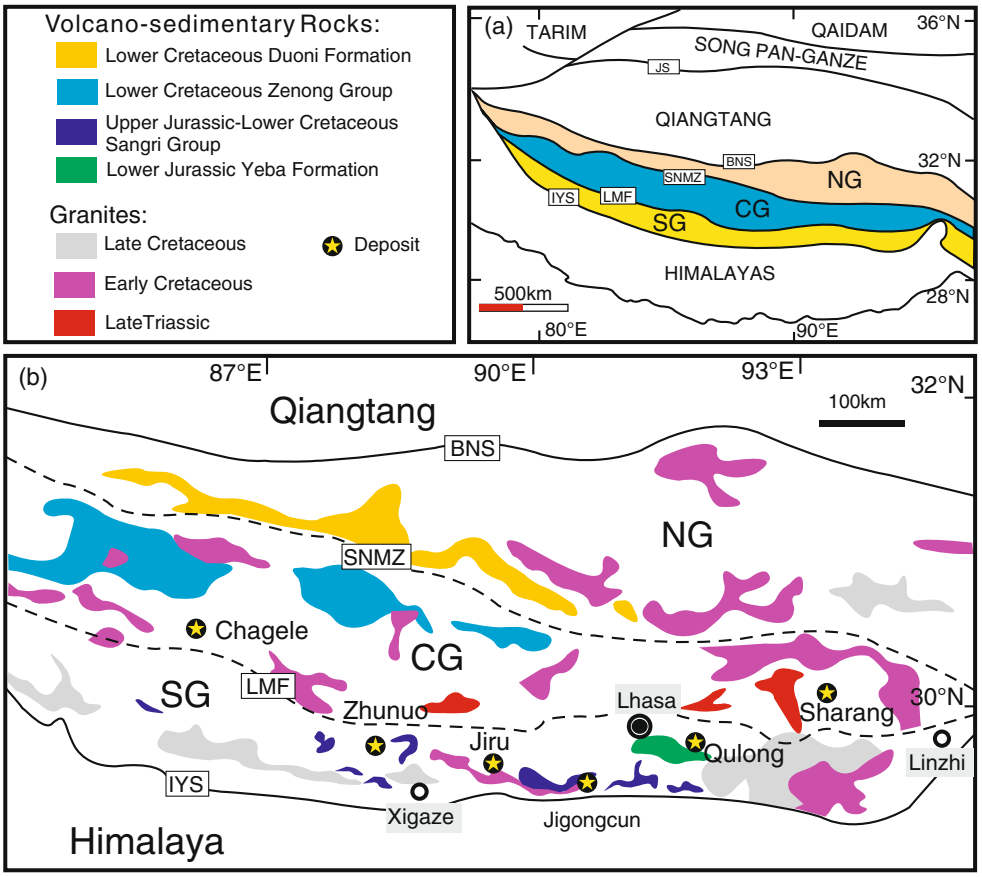

Fig. 1 Simplified tectonic framework of Gangdese belt showing locations of the molybdenum deposits, modified from Zhu et al. (2011). **a** Tectonic outline of the Tibetan Plateau showing the study area. **b** Simplified geological maps of the Tibetan-Himalayan orogen showing distribution of granite and volcano-sedimentary rocks. *Stars* indicate deposit locality. *JS* Jinsha Suture zone, *BNS* Bangong-Nujiang suture zone, *SNMZ* Shiquan River-Nam Tso Melange zone, *LMF* Luobadui-Milashan fault, *IYS* Indo-Yarlung sutures, *NG* north Gangdese belt, *CG* central Gangdese belt, *SG* south Gangdese belt

granite porphyries, of which the no. 1 is the most economically important. SHRIMP zircon U-Pb dating indicated magma emplaced at 15.6±0.6 Ma (Zheng et al. 2007). Potassic and phyllitic alterations are well developed within the porphyries, with minor clay mineral and carbonate alterations in places. Cu-Mo mineralization took place at 13.7±0.6 Ma as constrained by molybdenite Re-Os dating (Zheng et al. 2007), slightly younger than the zircon U-Pb age of the ore-hosting intrusion.

The Sharang porphyry Mo deposit lies in the north of the eastern Gangdese metallogenic belt, approximately 200 km northeast of Lhasa. The deposit is hosted in a stock-like granite porphyry in the southern part of the Sharang intrusive complex, which intrudes into the Upper Permian Mengla Formation (Zhao et al. 2012). The intrusive complex consists of pre-ore diorite, quartz diorite and granite, ore-related granite porphyries, and post-ore dikes of granitic composition. Laser ablation ICP-MS zircon U-Pb dating constrains the emplacement of two ore-related porphyries at 53.7±0.4 and 53.2 ±0.4 Ma, respectively (Zhao et al. 2014). Molybdenum mineralization consists of (1) quartz + molybdenite veins, (2) quartz + sulfide ± sulfate, (3) quartz-molybdenite stockworks, and (4) disseminations in hydrothermal cements of breccias of granite porphyry. Mo ores are mostly hosted in potassic and quartz-sericitie alterations (Zhao et al. 2014, 2015). Molybdenite Re-Os isochron age is 52.3±0.4 Ma, consistent with the zircon U-Pb age of the ore-related porphyries (Zhao et al. 2014).

The Qulong porphyry Cu-Mo deposit is the largest porphyry Cu deposit in China with more than 10 Mt contained Cu (Yang et al. 2009). It is situated in Maizhokunggar County, 84 km east of Lhasa in the eastern Gangdese metallogenic belt. The ore-bearing granodiorite porphyry was emplaced into intermediate volcanic rocks and clastic sequence of the middle Jurassic Yeba Formation at ca. 16.4±0.4 Ma (Wang et al. 2006). A striking feature of the Qulong deposit is the extreme development of both magmatic and hydrothermal anhydrite indicating high oxygen fugacity. The hydrothermal anhydrite commonly form veins with multiple sulfide mineral (molybdenite, chalcopyrite, pyrite), silicates (K-feldspar, sericite, chlorite), quartz, and carbonatite (Yang et al. 2009; Xiao et al. 2011; Hu et al. 2015). Four molybdenite separates have Re-Os model ages ranging from 16.8 to 15.8 Ma (Wang et al. 2006).

The Jigongcun Mo deposit lies in Quxu County, about 100 km southwest of Lhasa, in the central-south section of the Gangdese metallogenic belt. Magmatic intrusions in the mine consist of granodiorite and minor diorite and lamprophyre, which intrude tuff and marine tuffaceous sandstone and carbonates of the Lower Cretaceous Bima

Formation. Mineralization is dominated by quartz-molybdenite veins in granodiorite, with minor molybdenite disseminations in hydrothermal alteration haloes on both sides of the veins (Zhang et al. 2013). The veins are localized mainly in NW-striking faults cutting the host granodiorite. The formation age of the Jigongcun deposit was constrained at 22.3~22.8 Ma by molybdenite Re-Os dating (Zhang et al. 2013). Although Jigongcun differs from the above-mentioned porphyry Mo deposits in terms of hydrothermal alteration and mineralization styles, synthesis of regional geological and geochronological data indicates that the molybdenite veins formed from hydrothermal fluids exsolved from early Miocene magmas derived from partial melting of lower crust with minor input of mantle-derived melts under post-collisional setting. We therefore suggest that the Jigongcun deposit share common features with the other five porphyry Mo deposits about the tectonic setting and source of ore fluids and other components in the fluids.

Samples and analytical methods

Sampling

In total, 15 samples were collected for Mo isotope ratio measurements. Fourteen samples are from the molybdenite and 1 is from a quartz vein (Table 1). Fifteen magmatic rock samples from the ore-related intrusions in each deposit were taken for Nd isotope ratios (Table 2).

Mo isotope analysis

All molybdenite samples are free of alteration. Molybdenite was dissolved in aqua regia and reconstituted in 5 % HNO_3 without the need for pre-concentration or purification of Mo because of its high concentrations and lack of other major constituents (Barling et al. 2001). The molybdenite-quartz vein sample (JGC-1) was ground to fine powder (<200 mesh) in an agate mill. Sample preparation was carried out in a metal-free clean room fitted with an HEPA-filtered air supply and laminar low benches. 18 MΩ deionized "Milli-Q" water and ultra-pure acids (HCl and HNO_3) were used in the analyte purification, effectively reducing Mo blank and avoiding isobaric interferences of Zr and Ru (Zhou et al. 2015). About 120 mg powder of each sample was digested in Teflon containers with 1.5 mL HF and 1.5 mL HNO_3 acids at 190 °C for 48 h. Each 1.5 mL of HNO_3 was added and contents were evaporated to dryness to completely remove HF. Molybdenum was then purified by ion exchange resin Bio-Rad AGMP-1. The separation procedure followed the method of Siebert et al. (2006) modified by addition of 7 N HCl+0.03 % H_2O_2. Purified Mo fractions were evaporated to dryness and then diluted by 0.5 M HNO_3. This purification method can effectively eliminate matrix elements, including Zr and Ru. Mo recovery from the column separation was greater than 90 % (Zhou et al. 2012). Mo isotopic composition was determined by Neptune multi-collector inductively coupled plasma mass spectrometry (MC-ICP-MS) at State Key Laboratory of Geological Processes and Mineral Resources, China University of Geosciences, Wuhan. Typical operational conditions for the instrument and the Mo isotope ratio measurements are described in Archer and Vance (2008). An external normalization technique of ^{97}Mo-^{100}Mo double spike was used to correct the instrumental mass bias (Siebert et al. 2001). Mo isotope compositions are reported relative to a Johnson Matthey ICP standard solution, where $\delta^{97}Mo=[(^{97}Mo/^{95}Mo)_{sample}/(^{97}Mo/^{95}Mo)_{standrad}-1]\times 1000$ and the deviation obtained is less than 0.05‰. The standard material of Johnson Matthey ICP standard solution (lot 602332B) used in this study is similar to the Johnson Matthey Specpure Molybdenumas standard adopted by Mathur et al. (2010). Therefore, the data from the two laboratories are comparable. As demonstrated by Wen et al. (2010), different standard materials have no significant effect on the Mo isotope ratio results. To validate the analytical procedure, replicate analysis of SDO-1 (n=4) were performed. Results for $\delta^{97}Mo$ are in a narrow range between 0.70±0.04‰ (2s) and 0.79±0.03‰ (2s) for four replicates of SDO-1, with a mean value of 0.73±0.09‰ (2s), which is in good agreement with previously determined Mo isotope data of SDO-1 (Poulson-Brucker et al. 2009; Duan et al. 2010; Scheiderich et al. 2010; Goldberg et al. 2013). In order to facilitate data comparisons, we converted all literature-derived Mo isotope data in this study to $\delta^{97}Mo$ based on $\delta^{97}Mo=2/3\times\delta^{98}Mo$ (Barling et al. 2001). In addition, two samples were analyzed in duplicate with reproducibility typically better than 0.08‰ (2s) (Table 2). These results confirm the accuracy of the analytical procedure employed for the determination of Mo ratios.

Nd isotope analysis

The magmatic rocks associated with mineralization were ground to smaller than 200 mesh in an agate mill. About 120 mg powder from each sample was digested in Teflon containers with mixed HF and HNO_3 acids at 190 °C for 48 h. Neodymium was then purified by ion exchange resin AG50×8 and LN. Sample blank of this separation process were minimum (<0.1 ng). Neodymium isotopic compositions were determined by thermal ionization mass spectrometry (TRITON) at State Key Laboratory of Geological Processes and Mineral Resources, China University of Geosciences, Wuhan. The BCR-2 and JNdi-1 standards have $^{143}Nd/^{144}Nd$ ratios of 0.512643±0.000015 and 0.512116±0.000008 (2σ), respectively, using $^{146}Nd/^{144}Nd=0.721900$ for the correction of instrument mass fractionation were obtained for.

Table 1 Information and Mo isotopic compositions of samples

Sample	Location	Description	Lithology	δ^{97}Mo/‰	2s	Re/ppm	Re-Os/Ma	References (Re contents and Re-Os age)
CGL-1	Chagele deposit, Tibet	Porphyry Cu-Mo deposit; Qz-Mol-Ccp-Lm vein host by granite porphyry	Molybdenite	0.85	0.03	3.37	61.37	Gao et al. 2012
CGL-2	Chagele deposit, Tibet	Porphyry Cu-Mo deposit; Qz-Mol-Ccp-Lm vein host by granite porphyry	Molybdenite	0.88	0.03	5.21	62.15	Gao et al. 2012
ZN-1	Zhunuo deposit, Tibet	Porphyry Cu deposit; disseminated Mol-Ccp vein host by monzonitic granite porphyry	Molybdenite	0.10	0.02	227.15	13.99	Zheng et al. 2007
ZN-2	Zhunuo deposit, Tibet	Porphyry Cu deposit; disseminated Mol-Ccp vein host by monzonitic granite porphyry	Molybdenite	−0.09	0.02	312.11	13.98	Zheng et al. 2007
ZN-3	Zhunuo deposit, Tibet	Porphyry Cu deposit; disseminated Mol-Ccp vein host by monzonitic granite porphyry	Molybdenite	−0.07	0.02	292.99	13.83	Zheng et al. 2007
SR-1	Sharang deposit, Tibet	Porphyry Mo deposit; stockwork Qz-Mol vein host by granite porphyry	Molybdenite	0.05	0.03	74.23	51.85	Tang et al. 2009
SR-2	Sharang deposit, Tibet	Porphyry Mo deposit; stockwork Qz-Mol vein host by granite porphyry	Molybdenite	0.05	0.01	67.95	51.57	Tang et al. 2009
SR-3	Sharang deposit, Tibet	Porphyry Mo deposit; Qz-Mol-Py vein host by granite porphyry	Molybdenite	−0.01	0.01	56.81	52.29	Tang et al. 2009
QL	Qulong deposit, Tibet	Porphyry Cu deposit; Qz-Ccp-Mol-Py vein host by granite porphyry	Molybdenite	−0.13	0.03	615.40	16.21	Meng et al. 2003
JR	Jiru deposit, Tibet	Porphyry Cu deposit; Qz-Ccp-Mol-Py vein host by biotite monzonitic granite	Molybdenite	0.04	0.04	81.87	48.15	Zhang et al. 2008
JGC	Jigongcun deposit, Tibet	Vein-type deposit, Qz-Mol vein hosted in granodiorite	Molybdenite	−0.48	0.03	1514	22.29	Zhang et al. 2013
JGC-1	Jigongcun deposit, Tibet	Vein-type deposit, Qz-Mol vein hosted in granodiorite	Quartz vein	−0.58	0.01			
Bingham	Bingham deposit, American	Porphyry Cu-Mo deposit; qtz vein with coarse-grained Mol-Ccp-Py hosted in rhyolite porphyry	Molybdenite	0.46	0.02			
El Teniente	El Teniente deposit, Chile	Porphyry Cu-Mo deposit; Qz-Mol-Ccp vein hosted in tonalite porphyry	Molybdenite	0.27	0.03			
Henderson	Henderson deposit, American	Porphyry Cu-Mo deposit; Qz-Mol vein hosted in ivernite	Molybdenite	−0.10	0.03			
Duplicate data								
Bingham			Molybdenite	0.43	0.02			
El Teniente			Molybdenite	0.21	0.02			

Qz quartz, *Mol* molybdenite, *Ccp* chalcopyrite, *Lm* limonite, *Py* pyrite

Results

Results of molybdenum isotope ratios are presented in Table 1. Molybdenite samples from the porphyry Mo deposits in the Gangdese metallogenic belt have the δ^{97}Mo ranging from −0.09 to 0.88‰. The results are similar to those obtained in previous studies for molybdenite of porphyry systems (−0.53 to 0.53‰) (Pietruszka et al. 2006; Hannah et al. 2007; Mathur et al. 2010). Molybdenite from the Henderson porphyry Mo deposit shows a slightly negative δ^{97}Mo value of −0.10‰. Molybdenite samples from the El Teniente and Bingham porphyry Cu-Mo deposits yield δ^{97}Mo values of 0.27 and 0.46‰, respectively. The δ^{97}Mo value of the El Teniente deposit is indistinguishable from the results reported by Mathur et al. (2010) (−0.16, 0.15, 0.27, and 0.34‰). Molybdenite (JGC) and quartz vein (JGC-1) from Jigongcun deposit show negative δ^{97}Mo values of −0.48 and −0.58‰, respectively (Table 1).

The Nd isotope data of magmatic rocks associated with mineralization are given in Table 2. They have a wide $\varepsilon_{Nd}(t)$ values ranging from −18.66 to 2.96. Two samples from Chagele has lower $\varepsilon_{Nd}(t)$ values from −12.12 to −12.28. The Nd isotopes in Zhuonuo, Sharang, Qulong, and Jiru show large variations, with $\varepsilon_{Nd}(t)$ changing from −3.23 to −7.23. The granite porphyry from Qulong has a higher $\varepsilon_{Nd}(t)$ value of −1.05. The quartz vein and diorite from Jigongcun deposit

Table 2 Nd isotopic compositions of magmatic rocks associated with mineralization

Sample	Lithology	Age/Ma[a]	Sm/ppm	Nd/ppm	$^{147}Sm/^{144}Nd$	$^{143}Nd/^{144}Nd$[b]	$\varepsilon_{Nd}(t)$
CGL-1	Quartz vein	63	0.17	0.82	0.1225	0.511978(08)	−12.28
CGL-2	Granite porphyry	63	5.82	28.53	0.1129	0.511982(06)	−12.12
ZN-1	Granite porphyry	13	5.63	31.03	0.1099	0.512332(02)	−5.82
ZN-2	Granite porphyry	13	3.35	22.40	0.0904	0.512259(17)	−7.21
ZN-3	Granite porphyry	13	2.76	16.46	0.1017	0.512259(06)	−7.23
SR-1	Granite porphyry	53	4.47	27.42	0.0988	0.512376(11)	−4.45
SR-2	Granite porphyry	53	4.45	27.72	0.0971	0.512407(10)	−3.83
SR-3	Granite porphyry	53	4.50	27.21	0.1001	0.512370(08)	−4.58
QL	Granite porphyry	16	2.57	15.12	0.1697	0.512578(09)	−1.05
JR	Biotite monzonitic granite	48	2.57	15.90	0.1617	0.512443(06)	−3.23
JGC-1	Quartz vein	22	0.10	0.35	0.1692	0.512605(11)	−0.57
JGC-2	Granodiorite	22	2.97	14.90	0.1206	0.512779(05)	2.96
Bingham	Rhyolite porphyry	39	5.16	32.18	0.0972	0.511747(03)	−16.88
Henderson	Ivernite	27	4.21	23.98	0.1063	0.511665(12)	−18.66
El Teniente	Tonalite porphyry	5	1.28	6.08	0.1278	0.512786(04)	2.94

The initial ε_{Nd} values were calculated

[a] Ages data from Geissman et al. 1992, Deino and Keith 1997, Maksaev et al. 2004, Wang et al. 2006, Zheng et al. 2007, Zhang et al. 2008, Gao et al. 2012, and Zhao et al. 2012

[b] Data in the bracket is presented as two sigma of the mean, for data measurement procedure, see text

$$\varepsilon_{Nd}(t) = \left[\left(^{143}Nd/^{144}Nd\right)_t/\left(^{143}Nd/^{144}Nd\right)_{CHUR,t}-1\right] \times 10000 ;$$
$$\text{Where } \left(^{143}Nd/^{144}Nd\right)_{CHUR,t} = \left(^{143}Nd/^{144}Nd\right)_{CHUR,0}-\left(^{147}Sm/^{144}Nd\right)_{CHUR,0} \times \left(e^{\lambda t}-1\right);$$
$$\left(^{143}Nd/^{144}Nd\right)_t = \left(^{143}Nd/^{144}Nd\right)_0- \left(^{147}Sm/^{144}Nd\right)_0 \times \left(e^{\lambda t}-1\right) ;$$
$$\left(^{143}Nd/^{144}Nd\right)_{CHUR,0} = 0.512638,\ \left(^{147}Sm/^{144}Nd\right)_{CHUR,0} = 0.1967,\ \lambda = 6.54 \times 10^{-12}.$$

yields $\varepsilon_{Nd}(t)$ value of −0.57 and 2.96, respectively. The Henderson and Bingham character has a low $\varepsilon_{Nd}(t)$ value of −18.66 and 16.88, respectively. Tonalite porphyry from El Teniente has $\varepsilon_{Nd}(t)$ value of 2.94.

Discussion

Mo isotope fractionation in ore-forming process

The quartz vein (JGC-1) and molybdenite samples (JGC) from the Jigongcun deposit have comparable $\delta^{97}Mo$ values (−0.58 and −0.48‰, respectively), indicating that there is no significant fractionation of Mo isotopes during the precipitation of molybdenite. Similar observations are also found between sulfide ores and ore-hosting black shale in the early Cambrian Ni-Mo-PGE-Au polymetallic mineralization in South China: the ores and host rocks have similar Mo isotopes (0.94 to 1.38‰ and 0.81 to 1.70‰, respectively) (Xu et al. 2012, 2013). These observations suggest that ore-forming temperature is not the main factor for Mo isotope fractionation in molybdenite (Hannah et al. 2007). Similarly, igneous rocks formed under high-T and high-P conditions define a narrow range of $\delta^{97}Mo$ values from −0.06 to 0.17‰ (Siebert et al. 2003), which suggests that magmatic process does not cause measurable Mo isotope fractionation.

Influence of tectonic setting and source on Mo isotopes in molybdenite

Porphyry copper-molybdenum deposits were formed in two contrast tectonic settings: oceanic subduction and collisional orogenesis. The former is best represented by porphyry systems in the Pacific Rim porphyry deposits (Cooke et al. 2005), and the latter by the Gangdese metallogenic belt (Hou et al. 2009). The porphyry copper-molybdenum deposits are generally derived from high oxygen fugacity magmas (Seedorff et al. 2005). Therefore, the Mo isotope fractionation caused by different redox conditions can be reduced in the process of mineralization.

Porphyry Cu-Mo deposits in the Gangdese metallogenic belt formed in three separate mineralizing episodes under different tectonic settings since the India-Asia convergence (Hou et al. 2009). Molybdenite Re-Os dating revealed that the Chagele, Sharang, and Jiru deposits formed in the early Cenozoic (62–48 Ma), coinciding with the India-Asia continental collision beginning at ca. 65 Ma (Table 1). The other porphyry Mo deposits were emplaced at 16–15 Ma (Qulong;

Wang et al. 2006) and 14–13 Ma (Zhunuo; Zheng et al. 2007) related to post-collisional extension. Two samples (CGL-1, CGL-2) from the Chagele deposit have positive values of δ^{97}Mo (0.85 and 0.88‰, respectively), coupled with a low initial $\varepsilon_{Nd}(t)$ value of −12.28 and −12.12, respectively. In contrast, samples from other porphyry deposits in the Gangdese belt (Sharang, Jiru, Zhuonuo, and Qulong) have significantly lower δ^{97}Mo values (−0.13 ~ 0.10‰), coupled with higher $\varepsilon_{Nd}(t)$ values (−7.23 ~ −1.05).

Syn-collisional setting

The Chagele and Sharang deposits in the Central Gangdese metallogenic belt formed under syn-collisional setting (65 ~ 38 Ma) during collision of the Indian and Eurasian continents in the early Paleogene (Hou et al. 2009). Geochemical and isotopic compositions of granitoid intrusions indicate that the deposits and surrounding areas are underlain by ancient lower crust basement. The Nd isotopic compositions of the ore-bearing porphyry imply distinct sources for the ore-related magmas (Table 2). The ore-bearing porphyry at Chagele has a similar Nd isotopic composition with old lower crust ($\varepsilon_{Nd}(t)$=−12.5; Hou et al. 2013) in Tibet. However, its $\varepsilon_{Hf}(t)$ values and peraluminous nature indicate that the magma was derived from the melting of upper crust sediments (Wang et al. 2012). The porphyry at Chagele likely have the same source as the 90 ~ 120 Ma granites (Zhu et al. 2011), which are related to northward subduction of Neo-Tethys in Central Gangdese. In contrast, the Sr-Nd isotopes ($(^{87}Sr/^{86}Sr)_I$= 0.706111 ~ 0.707096 and $\varepsilon_{Nd}(t)$=−4.59 ~ −3.37) of porphyry related to the Sharang deposit indicate that ore-bearing magma may have formed by melting the metasomatised mantle wedge following mixing between the mantle-derived magmas and old continental crust at lower crust (Zhao et al. 2012). The Jiru deposit in the Southern Gangdese, also considered to be syn-collisional and sourced from juvenile lower crust, has Mo and Nd isotopic compositions similar to the values of the Sharang deposit.

Post-collisional setting

Miocene magmatic activity (26 ~ 10 Ma) in the Gangdese metallogenic belt has been interpreted to occur under a post-collisional extensional environment. The ore-bearing porphyries at Qulong and Zhunuo deposits have more positive $\varepsilon_{Nd}(t)$ values than the ancient lower crust of Tibet. This indicates that the magmas were derived from juvenile lower crust, and mixed with mantle-derived melts (Hou et al. 2013). Moreover, the Qulong porphyry was mainly sourced from mantle with little crust contamination. Molybdenite from Qulong is more enriched in lighter Mo isotopes relative to the Zhuonuo deposit. Thus, Mo isotope ratios of molybdenite appear to be more dependent on the source of the ore-related magmas rather than tectonic setting under which the deposits formed. The Sharang, Jiru, and Zhuonuo Cu-Mo deposits, which share a common source dominated by lower crust and upper mantle, have similar Mo isotopes (δ^{97}Mo≈0‰). This is consistent with the tertiary granite from Himalaya (δ^{97}Mo= 0.09 ‰; Siebert et al. 2003). The Chagele deposit is enriched in heavy Mo isotope, consistent with an upper crustal affiliation of the mineralized porphyry. The continental sediments have a large range of Mo isotopic compositions, with δ^{97}Mo values from −0.34 to 0.80‰ (Siebert et al. 2006) in continental margin marine sediments and from 0 to 1.70‰ in rivers (Archer and Vance 2008; Pearce et al. 2010). Therefore, the positive δ^{97}Mo values of the Chagele deposit likely reflect addition of upper crustal materials with high δ^{97}Mo in the Mo-bearing magmas. The Qulong and Jigongcun deposits are enriched in light Mo isotope, consistent with the predominant mantle source for the magmas. The Henderson porphyry Mo deposit is genetically related to crustally-derived porphyries in post-collisional extension environment on the western margin of the North American craton (Sinclair 2007). The Mo isotopes (δ^{97}Mo=−0.10‰) of molybdenite from the Henderson deposit is consistent with values of porphyry Cu-Mo deposits sourced from lower crust with minor contributions of mantle in the Gangdese belt.

Oceanic subduction setting

The El Teniente and Bingham porphyry Cu-Mo deposits are genetically associated with oceanic subduction. Molybdenite from these deposits is enriched in heavy Mo isotope. The mineralized porphyry at El Teniente has an adakite affinity and high $\varepsilon_{Nd}(t)$ values, indicating an origin by partial melting of the subducted Juan Fernandez Rige (Skewes and Stern 1994, 1995). The δ^{97}Mo values (−0.16 to 0.34‰; Hannah et al. 2007) of molybdenite from the El Teniente deposit have a similar range to that from the Los Pelambres deposit (0.00 to 0.25‰; Hannah et al. 2007; Mathur et al. 2010), which is also associated with oceanic subduction in Chile. Generation of the late Eocene Bingham deposit (Redmond et al. 2004) has been related to the retreat of the Farallon Plate that caused rising of hot asthenospheric mantle and consequently melting of the lithospheric mantle (Maughan et al. 2002). The low $\varepsilon_{Nd}(t)$ values of the ore-bearing porphyry at Bingham reflect a significant crustal assimilation of the parental magma during its ascent. Molybdenite from the Bingham deposit has δ^{97}Mo value (0.46‰) slightly higher than that from Los Pelambres and El Teniente in Chile, as for the Chagele deposit in the Gangdese belt. In summary, Mo isotopic compositions of molybdenite are a good indicator for the source of mineralized porphyry, but without direct link to the age of the deposit or the tectonic setting of the deposits formed.

An integrated tracer using Re contents and Nd isotopes

Rhenium and molybdenum have common geochemical characteristics. Therefore, Re can be preferentially incorporated into the lattice structure of molybdenite, and thus can be used as a signature for the source of Mo (Stein et al. 2001). Based on a statistical study of Mo deposits in China, Mao et al. (1999) suggested that molybdenite related to mantle-derived magmas generally has the highest Re contents, whereas the varieties related to hybrid magma and crustally-derived melts have progressively lower Re contents. Figure 2 shows a negative correlation between Mo isotopic compositions and rhenium contents in molybdenite. Molybdenite tends to enrich in heavier Mo isotopes with decreasing Re contents. Molybdenite from the Chagele deposit, which is related to crustally-sourced magmas, has positive δ^{97}Mo values and the lowest Re concentrations. The opposite observations of the Jigongcun and Qulong deposits are related to mantle-derived magmas, with negative δ^{97}Mo values and the highest Re contents. The Sharang, Jiru, and Zhunuo deposits, characterized by a hybrid magma, have δ^{97}Mo (≈0‰) and Re contents intermediate to the above-mentioned two end-members. The variation in Mo isotopic compositions of molybdenite from the porphyry Cu-Mo deposits in the Gangdese belt and the source of the ore-related magmas also reflect tectonic evolution at different stages. In the beginning of continental collision, partial melting of crustal materials played an important role in forming the Paleogene magmatic intrusions, molybdenite sourced from which contained low Re and positive δ^{97}Mo values. In contrast, the Miocene Mo-mineralized porphyries formed under post-collisional extension environment and have an enriched mantle-like signature. Consequently, molybdenite has the highest Re but is characteristically low in δ^{97}Mo value. The relationship between Mo isotopes and Re contents

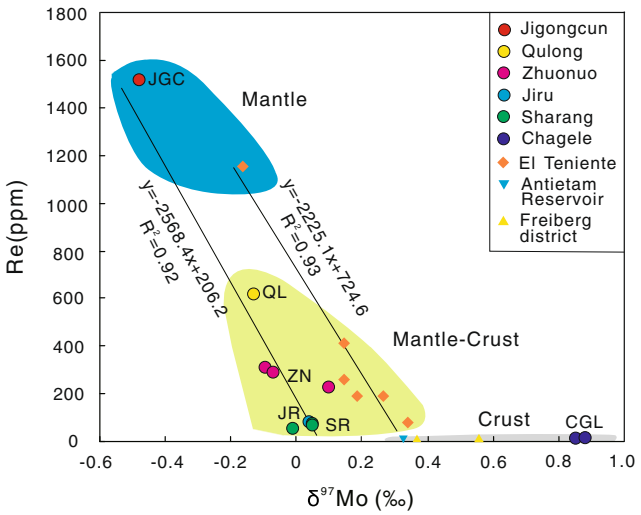

Fig. 2 Plot of the Re concentration versus δ^{97}Mo in molybdenites. The data of *triangle* and *diamond* from Mathur et al. (2010)

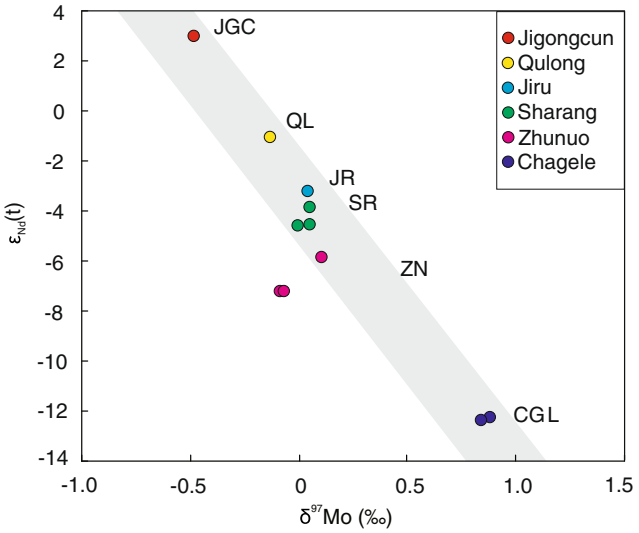

Fig. 3 Plot of the $\varepsilon_{Nd}(t)$ in magmatic rocks associated with mineralization versus δ^{97}Mo of molybdenites

in molybdenites has also been studied by Mathur et al. (2010). In their study, the δ^{97}Mo values of six molybdenite samples from the El Teniente porphyry Cu-Mo deposits range from −0.16 to 0.34‰. These samples show a negative correlation (R^2=0.93) between Re contents and δ^{97}Mo (Fig. 2). The most likely interpretation for these observations is the magma source from which Mo is derived, rather than the Rayleigh fractionation during ore-forming processes as suggested by Hannah et al. (2007).

The Re contents in molybdenite are controlled by the partition between vapor and liquid during phase separation of the ore fluids. It may also be affected by the mineral assemblages coexisting with molybdenite. Hence, molybdenite coexisting with wolframite would have low Re contents; however, the molybdenite associated with chalcopyrite and magnetite are expected to contain high Re (Stein et al. 2001). Figure 3 schematically illustrates the negative correlations between δ^{97}Mo of molybdenite and $\varepsilon_{Nd}(t)$ values of magmatic rocks related to porphyry Cu-Mo mineralization investigated in this study. The lower $\varepsilon_{Nd}(t)$ value of ore-related porphyry at Chagele (with a high δ^{97}Mo value) reflects the predominance of crustal materials as the potential source for the porphyry. The host diorite of the Jigongcun deposit has $\varepsilon_{Nd}(t)>0$ corresponding to much lower δ^{97}Mo.

Conclusions

The collision origin porphyry molybdenites in Sharang, Jiru, Qulong, and Zhunuo of Gangdese belt have similar δ^{97}Mo (~0‰). However, a relatively high δ^{97}Mo (0.85~0.88‰) and low δ^{97}Mo (−0.48 %) are found in Chagele and Jigongcun, respectively. The relationship between Nd isotope of magmatic rock and the Mo isotope of molybdenites in

Gangdese belt suggests that the change of the Mo isotope compositions is mainly related to the magma source, rather than the tectonic setting. The Mo isotope and Re concentrations in molybdenites have a negative correlation. Molybdenite from crustal sources has relatively positive δ^{97}Mo values. On the contrast, molybdenite from the mantle sources has a negative δ^{97}Mo value. Mo isotope of molybdenites is a good indicator for the source of mineralized porphyry.

Acknowledgments We wish to thank Dr. Yunxing Xue from the Department of Geology, Australian National University, and Prof. Zheng Youye from China University of Geosciences for their invaluable help in sample collection and associated fieldwork. We thank Georges Beaudoin (Editor-in-Chief) and Rolf Romer (Associate editor) for editorial handling and an anonymous reviewer for his/her reviews which considerably improved an earlier version of this manuscript. This study has been supported financially by the National Natural Science Foundation of China (nos. 41073007, 41273005, 41473007), the Ministry of Education of China (IRT0441 and B07039), and the MOST Special Fund from the State Key Laboratory of Geological Processes and Mineral Resources.

References

Archer C, Vance D (2008) The isotopic signature of the global riverine molybdenum flux and anoxia in the ancient oceans. Nat Geosci 1: 597–600

Arnold GL, Anbar AD, Barling J, Lyons TW (2004) Molybdenum isotope evidence for widespread anoxia in mid-Proterozoic oceans. Science 304:87–90

Barling J, Arnold GL, Anbar AD (2001) Natural mass-dependent variations in the isotopic composition of molybdenum. Earth Planet Sci Lett 193:447–457

Chu MF, Chung SL, Song B, Liu DY, O'Reilly SY, Pearson NJ (2006) Zircon U-Pb and Hf isotope constraints on the Mesozoic tectonics and crustal evolution of southern Tibet. Geology 34:745–748

Chung SL, Chu MF, Zhang YQ, Xie YW, Lo CH, Lee TY, Lan CY, Li XH, Zhang Q, Wang YZ (2005) Tibetan tectonic evolution inferred from spatial and temporal variations in post-collisional magmatism. Earth Sci Rev 68:173–196

Cooke DR, Hollings P, Walshe JL (2005) Giant porphyry deposits: characteristics, distribution, and tectonic controls. Econ Geol 100:801–818

Deino A, Keith JD (1997) Ages of volcanic and intrusive rocks in the Bingham mining district, Utah. Soc Econ Geol Guidebook Series 29:91–100

Ding L, Kapp P, Zhong D, Deng WM (2003) Cenozoic volcanism in Tibet: evidence for a transition from oceanic to continental subduction. J Petrol 44:1833–1865

Duan Y, Anbar AD, Arnold GL, Lyons TW, Gordon GW, Kendall B (2010) Molybdenum isotope evidence for mild environmental oxygenation before the Great Oxidation Event. Geochim Cosmochim Acta 74:6655–6668

Gao SB, Zheng YY, Tian LM, Zhang Z, Qu WJ, Liu MY, Zheng HT, Zheng L, Zhu JH (2012) Geochronology of magmatic intrusions and mineralization of Chagele copper-lead-zinc deposit in Tibet and its implications. Earth Sci J China Univ Geosci 37:507–514 **(in Chinese with English abstract)**

Geissman JW, Snee LW, Graaskamp GW, Carten RB, Geraghty EP (1992) Deformation and age of the Red Mountain intrusive system (Urad-Henderson molybdenum deposits), Colorado: evidence from paleomagnetic and ^{40}Ar/^{39}Ar data. Geol Soc Am Bull 104:1031–1047

Goldberg T, Gordon G, Izon G, Archer C, Pearce CR, McManus J, Anbar AD, Rehkämper M (2013) Resolution of inter-laboratory discrepancies in Mo isotope data: an intercalibration. J Anal Atom Spectrom 28:724–735

Hannah JL, Stein HJ, Wieser ME, de Laeter JR, Varner MD (2007) Molybdenum isotope variations in molybdenite: vapor transport and Rayleigh fractionation of Mo. Geology 35:703–706

Hou ZQ, Yang ZM, Qu XM, Meng XJ, Li ZQ, Beaudoin G, Rui ZY, Gao YF (2009) The Miocene Gangdese porphyry copper belt generated during post-collisional extension in the Tibetan Orogen. Ore Geol Rev 36:25–51

Hou ZQ, Zheng YC, Yang ZM, Rui ZY, Zhao ZD, Jiang SH, Qu XM, Sun QZ (2013) Contribution of mantle components within juvenile lower-crust to collisional zone porphyry Cu systems in Tibet. Miner Deposita 48:173–192

Hu YB, Liu JQ, Ling MX, Ding W, Liu Y, Zartman RE, Ma XF, Liu DY, Zhang CC, Sun SJ, Zhang LP, Wu K, Sun WD (2015) The formation of Qulong adakites and their relationship with porphyry copper deposit: geochemical constraints. Lithos 220–223:60–80

Lehmann B, Nägler TF, Holland HD, Wille M, Mao JW, Pan JY, Ma DS, Dulski P (2007) Highly metalliferous carbonaceous shale and Early Cambrian seawater. Geology 35:403–406

Maksaev V, Munizaga F, McWilliams M, Fanning M, Mathur R, Ruiz J, Zentilli M (2004) New chronology for El Teniente, Chilean Andes, from U/Pb, ^{40}Ar/^{39}Ar, Re/Os and fission-track dating: implications for the evolution of a supergiant porphyry Cu-Mo deposit. In: Sillitoe RH, Perello J, Vidal CE (eds) Andean metallogeny: new discoveries, concepts, and updates. SEG special publication 11. Society of Economic Geologists, White Plains, pp 15–54

Malinovsky D, Hammarlund D, Ilyashuk B, Martinsson O, Gelting J (2007) Variations in the isotopic composition of molybdenum in freshwater lake systems. Chem Geol 236:181–198

Mao JW, Zhang ZC, Zhang ZH, Du AD (1999) Re-Os isotopic dating of molybdenites in the Xiaoliugou W (Mo) deposit in the northern Qilian mountains and its geological significance. Geochim Cosmochim Acta 63:1815–1818

Mathur R, Brantley S, Anbar A, Munizaga F, Maksaev V, Newberry R, Vervoot J, Hart G (2010) Variation of Mo isotopes from molybdenite in high-temperature hydrothermal ore deposits. Miner Deposita 45: 43–50

Maughan DT, Keith JD, Christiansen EH, Pulsipher T, Hattori K, Evans NJ (2002) Contributions from mafic alkaline magmas to the Bingham porphyry Cu-Au-Mo deposit, Utah, USA. Miner Deposita 37:14–37

Meng XJ, Hou ZQ, Gao YF, Huang W, Qu XM, Qu WJ (2003) Re-Os dating for molybdenite from Qulong porphyry copper deposit in Gangdese metallogenic belt, Xizang and its metallogenic significance. Geol Rev 49:660–665 **(in Chinese with English abstract)**

Pearce CR, Cohen AS, Coe AL, Burton KW (2008) Molybdenum isotope evidence for global ocean anoxia coupled with perturbations to the carbon cycle during the Early Jurassic. Geology 36:231–234

Pearce CR, Burton KW, von Strandmann PA, James RH, Gislason SR (2010) Molybdenum isotope behaviour accompanying weathering and riverine transport in a basaltic terrain. Earth Planet Sci Lett 295: 104–114

Pietruszka AJ, Walker RJ, Candela PA (2006) Determination of mass-dependent molybdenum isotopic variations by MC-ICP-MS: an evaluation of matrix effects. Chem Geol 225:121–136

Poulson-Brucker RL, McManus J, Severmann S, Berelson WM (2009) Molybdenum behavior during early diagenesis: insights from Mo isotopes. Geochem Geophys Geosyst 10:1–25

Redmond PB, Einaudi MT, Inan EE, Landtwing MR, Heinrich CA (2004) Copper deposition by fluid cooling in intrusion-centered

systems: new insights from the Bingham porphyry ore deposit, Utah. Geology 32:217–220

Scheiderich K, Helz GR, Walker RJ (2010) Century-long record of Mo isotopic composition in sediments of a seasonally anoxic estuary (Chesapeake Bay). Earth Planet Sci Lett 289:189–197

Seedorff E, Dilles J, Proffett J, Einaudi M, Zurcher L, Stavast W, Johnson D, Barton M (2005) Porphyry deposits: characteristics and origin of hypogene features. Econ Geol 100th Ann 29:251–298

Siebert C, Nägler TF, Kramers JD (2001) Determination of molybdenum isotope fractionation by double-spike multicollector inductively coupled plasma mass spectrometry. Geochem Geophys Geosyst 2 paper number 2000GC000124

Siebert C, Nägler TF, Blanckenburg FV, Kramers JD (2003) Molybdenum isotope records as a potential new proxy for paleoceanography. Earth Planet Sci Lett 211:159–171

Siebert C, McManus J, Bice A, Poulson R, Berelson WM (2006) Molybdenum isotope signatures in continental margin marine sediments. Earth Planet Sci Lett 241:723–733

Sinclair WD (2007) Porphyry deposits. In: Goodfellow WD (ed) Mineral deposits of Canada: a synthesis of major deposit-types, district metallogeny, the evolution of geological provinces, and exploration methods. GAC Special Publication 5. Geological Association of Canada, St. John's, pp 223–243

Skewes MA, Stern CR (1994) Tectonic trigger for the formation of late Miocene Cu-rich breccia pipes in the Andes of central Chile. Geology 22:551–554

Skewes MA, Stern CR (1995) Genesis of the giant late Miocene to Pliocene copper deposits of central Chile in the context of Andean magmatic and tectonic evolution. Int Geol Rev 37:893–909

Stein HJ, Markey RJ, Morgan JW, Hannah JL, Scherstén A (2001) The remarkable Re–Os chronometer in molybdenite: how and why it works. Terra Nov. 13:479–486

Tang JX, Chen YC, Wang DH, Wang CH, Xu YP, Qu WJ, Huang W, Huang Y (2009) Re-Os dating of molybdenite from the Sharang porphyry molybdenum deposit in Gongboyamda county, Tibet and its geological significance. Acta Geol Sin 83:698–704 **(in Chinese with English abstract)**

Wang LL, Mo XX, Li B, Dong GC, Zhao ZD (2006) Geochronology and geochemistry of the ore-bearing porphyry in Qulong Cu (Mo) ore deposit, Tibet. Acta Petrol Sin 22:1001–1008 **(in Chinese with English abstract)**

Wang BD, Guo L, Wang LQ, Li B, Huang HX, Chen FQ, Duan ZM, Zeng QG (2012) Geochronology and petrogenesis of the ore-bearing pluton in Chagele deposit in middle of the Gangdese metallogenic belt. Acta Petrol Sin 28:1647–1662 **(in Chinese with English abstract)**

Wen HJ, Carignan J, Cloquet C, Zhu XK, Zhang YX (2010) Isotopic delta values of molybdenum standard reference and prepared solutions measured by MC-ICP-MS: proposition for delta zero and secondary references. J Anal Atom Spectrom 25:716–721

Wille M, Kramers JD, Nägler TF, Beukes NJ, Schröder S, Meisel T, Lacassie JP, Voegelin AR (2007) Evidence for a gradual rise of oxygen between 2.6 and 2.5 Ga from Mo isotopes and Re-PGE signatures in shales. Geochim Cosmochim Acta 71:2417–2435

Xiao B, Qin KZ, Li GM, Li JX, Xia DX, Chen L, Zhao JX (2011) Highly oxidized magma and fluid evolution of Miocene Qulong giant porphyry Cu-Mo deposit, southern Tibet, China. Resour Geol 62:4–18

Xu LG, Lehmann B, Mao JW, Nägler TF, Neubert N, Böttcher ME, Escher P (2012) Mo isotope and trace element patterns of Lower Cambrian black shales in South China: multi-proxy constraints on the paleoenvironment. Chem Geol 318–319:45–59

Xu LG, Lehmann B, Mao JW (2013) Seawater contribution to polymetallic Ni–Mo–PGE–Au mineralization in Early Cambrian black shales of South China: evidence from Mo isotope, PGE, trace element, and REE geochemistry. Ore Geol Rev 52:66–84

Yang ZM, Hou ZQ, White NC, Chang ZS, Li ZQ, Song YC (2009) Geology of post-collisional porphyry copper-molybdenum deposit at Qulong, Tibet. Ore Geol Rev 36:133–159

Yin A, Harrion TM (2000) Geologic evolution of the Himalayan-Tibetan orogen. Annu Rev Earth Planet Sci 28:211–280

Zhang GY, Zheng YY, Gong FZ, Gao SB, Qu WJ, Pang YC, Shi YR, Yin SY (2008) Geochronologic constraints on magmatic intrusions and minerlization of the Jiru porphyry copper deposit, Tibet, associated with continent-collisional process. Acta Petrol Sin 24:473–479 **(in Chinese with English abstract)**

Zhang SK, Zheng YY, Zhang GY, Gao SB, Sun X, Yu M, Guo JW, Xu J (2013) Geochronological constraints on Jigongcun quartz-vein type molybdenum deposit in Quxu county, Tibet. Miner Deposits 32: 641–648 **(in Chinese with English abstract)**

Zhao JX, Qin KZ, Li GM, Li JX, Xiao B, Chen L (2012) Geochemistry and petrogenesis of Granitoids at Sharang Eocene Porphyry Mo deposit in the main-stage of India-Asia continental collision, Northern Gangdese, Tibet. Resour Geol 62:84–98

Zhao JX, Qin KZ, Li GM, Jin LY, Xiao B, Chen L, Yang YH, Li C, Liu YS (2014) Collision-related genesis of the Sharang porphyry molybdenum deposits, Tibet: evidence from zircon U-Pb ages, Re-Os ages and Lu-Hf isotopes. Ore Geol Rev 56:312–326

Zhao JX, Qin KZ, Li GM, Cao MJ, Evans NJ, Mclnnes BA, Li JX, Xiao B, Chen L (2015) The exhumation history of collision-related mineralizing systems in Tibet: insights from thermal studies of the Sharang and Yaguila deposits, Central Lhasa. Ore Geol Rev 65: 1043–1061

Zheng YY, Zhang GY, Xu RK, Gao SB, Pang YC, Cao L, Du AD, Shi YR (2007) Geochronologic constraints on magmatic intrusions and mineralization of the Zhunuo porphyry copper deposit in Gangdese, Tibet. Chin Sci Bull 52:3139–3147

Zheng YY, Sun X, Gao SB, Zhao ZD, Zhang GY, Wu S, You ZM, Li JD (2014) Multiple mineralization events at Jiru porphyry copper deposit, southern Tibet: implications for Eocene and Miocene magma sources and resource potential. J Asian Earth Sci 79:842–857

Zhou L, Wignall PB, Su J, Feng QL, Xie SC, Zhao LS, Huang JH (2012) U/Mo ratios and $\delta^{98/95}$Mo as local and global redox proxies during mass extinction events. Chem Geol 324–325:99–107

Zhou L, Algeo TJ, Shen J, Hu ZF, Gong HM, Xie SC, Huang JH, Gao S (2015) Changs in marine productivity and redox conditions during the Late Ordovician Hirnantian glaciation. Palaeogeogr Palaeoclimatol Palaeoecol. doi:10.1016/j.palaeo.2014.12.012

Zhu DC, Mo XX, Niu YL, Zhao ZD, Wang LQ, Liu YS, Wu FY (2009) Geochemical investigation of Early Cretaceous igneous rocks along an east–west traverse throughout the central Lhasa Terrane, Tibet. Chem Geol 268:298–312

Zhu DC, Zhao ZD, Niu YL, Mo XX, Chung SL, Hou ZQ, Wang LQ, Wu FY (2011) The Lhasa Terrane: record of a microcontinent and its histories of drift and growth. Earth Planet Sci Lett 301:241–255